

Supporting Information

Iron Triad (Fe, Co, Ni) Ternary Phosphide Nanosheet Arrays as High-Performance Bifunctional Electrodes for Full Water Splitting in Basic and Neutral Conditions

*Zhe Zhang^a, Jinhui Hao^{a,b}, Wenshu Yang^{a,b}, and Jilin Tang^{*a}*

^a State Key Laboratory of Electroanalytical Chemistry, Changchun Institute of Applied Chemistry,
Chinese Academy of Sciences, Changchun 130022, People's Republic of China

E-mail: jltang@ciac.ac.cn. Tel/Fax: (+86) 431-85262734

^b University of Chinese Academy of Sciences, Beijing, 100049, People's Republic of China

Experimental Section

Chemicals. $\text{Ni}(\text{NO}_3)_2 \cdot 6\text{H}_2\text{O}$ and NaH_2PO_2 were purchased from Aladdin Aladdin Industrial Inc. (Shanghai, China). Polyvinylpyrrolidone (PVP, K30), $\text{Fe}(\text{NO}_3)_3 \cdot 9\text{H}_2\text{O}$, and $\text{Co}(\text{NO}_3)_2 \cdot 6\text{H}_2\text{O}$ were purchased from Shanghai Chemical Factory (Shanghai, China). NaNO_3 was purchased from Beijing Chemical Reagent Factory (Beijing, China). Platinum on carbon (20% Pt/C, Pt on Vulcan XC-72R carbon support) was purchased from Alfa Aesar. All the reagents were used as received without further purification. All aqueous solutions were prepared with Milli-Q water ($>18.2 \text{ M}\Omega \cdot \text{cm}$) from a Milli-Q Plus system (Millipore).

Apparatus. X-ray photoelectron spectroscopy (XPS) measurement was performed on an ESCALABMK II spectrometer (VG Co., United Kingdom) with Al $K\alpha$ ($h\nu = 1486.6 \text{ eV}$) X-ray radiation as the X-ray source for excitation. The energy step size for the binding energy (BE) values was 1 eV and 0.1 eV for survey spectrum and high resolution, respectively. X-ray diffraction (XRD) spectra was obtained on a D8 ADVANCE (Germany) using Cu $K\alpha$ (1.5406 \AA) radiation. Field emission scanning electron microscope (SEM) images were obtained on a Hitachi S-4800. Transmission electron microscopy (TEM) and high-resolution TEM (HRTEM) images were obtained with a TECNAI G₂ high-resolution transmission electron microscope (Holland) with an accelerating voltage of 200 kV. The sample for TEM characterization was prepared by placing a drop of prepared solution on carbon-coated copper grid and drying at room temperature. The compositions of $\text{Fe}_x\text{Co}_y\text{Ni}_z$ were determined by Inductively Coupled Plasma Optical Emission Spectrometer (ICP-OES, X Series 2, Thermo Scientific USA). In order to avoid the impact of Ni foam substrate, $\text{Fe}_x\text{Co}_y\text{Ni}_z$ was synthesized via electrodeposition on Ti substrate for ICP-OES characterization.

Synthesis of $\text{Fe}_x\text{Co}_y\text{Ni}_z\text{P}$. Samples were denoted as $\text{Fe}_x\text{Co}_y\text{Ni}_z\text{P}$, in which x, y, and z stand for the molar concentration of Fe^{3+} , Co^{2+} and Ni^{2+} in the electrolyte. $\text{Fe}_x\text{Co}_y\text{Ni}_z\text{P}$ was synthesized via electrodeposition of $\text{Fe}_x\text{Co}_y\text{Ni}_z\text{-LDH}$ nanosheets array on Ni foam followed by low-temperature phosphidation process. Ni foam was cut into pieces of $10 \times 30 \text{ mm}^2$ and ultrasonically cleaned in 3 M HCl for 15 min to

remove the NiO_x layer on the surface, and rinsed with Milli-Q water and absolute ethanol successively, then dried in air. The electrodeposition was performed on a CHI 660A electrochemical analyzer (CH Instruments, Inc., Shanghai) with a three-electrode configuration consisting of a platinum plate as counter electrode, a saturated Ag/AgCl as reference electrode and Ni foam as working electrode. A 50 mL mixed solution of 30 mM Fe(NO₃)₃·9H₂O, 30 mM Co(NO₃)₂·6H₂O, 30 mM Ni(NO₃)₂·6H₂O, and 100 mg PVP was used as electrolyte bath. To optimize the compositions of the Fe_xCo_yNi_z deposit, the total moles of Fe³⁺, Co²⁺ and Ni²⁺ in the electrolyte were maintained at 90 mM while the molar ratio of Fe³⁺, Co²⁺ and Ni²⁺ was systematically varied. At the same time, the total moles of NO₃⁻ in the electrolyte were maintained at 210 mM using of NaNO₃. The constant potential electrodeposition was then carried out at -1.0V (versus saturated Ag/AgCl) at room temperature. The optimized deposition time of Fe_xCo_yNi_z has been determined to be 300 s. After electrodeposition, the Fe_xCo_yNi_z was carefully withdrawn from the electrolyte, rinsed with Milli-Q water and ethanol, then sonicated for 20 s in ethanol and left dry in air. The obtained Fe_xCo_yNi_z was transferred into a tubular furnace for phosphidation under N₂ gas. Two pieces of Fe_xCo_yNi_z and 500 mg NaH₂PO₂ were put at two separate positions in a fused silica tube with NaH₂PO₂ at the upstream side of the tubular furnace. Then the Fe_xCo_yNi_z was heated to 300 °C in N₂ gas and maintained at this temperature for 1 h with a heating rate of 3 °C min⁻¹. Black Fe_xCo_yNi_zP was obtained after cooled to room temperature under N₂ gas. For Fe₁₀Co₄₀Ni₄₀P electrode, the loading mass of Fe₁₀Co₄₀Ni₄₀P is about 3.1 mg cm⁻².

Electrochemical Measurements: Electrochemical measurements were performed on a CHI 660A electrochemical analyzer (CH Instruments, Inc., Shanghai). Electrochemical measurements were performed in a conventional three-electrode system using Fe_xCo_yNi_zP-Ni foam as the working electrode, saturated calomel electrode (SCE) as the reference electrode and carbon rod as the counter electrode. The potential, measured against a SCE electrode, was converted to the potential versus the reversible hydrogen electrode (RHE) according to $E_{vs\ RHE} = E_{vs\ SCE} + 0.242 + 0.059pH$. To prepare the Pt/C loaded electrode, Pt/C (18.6 mg) and 10 μL

polytetrafluoroethylene (PTFE 10 wt%) were dispersed in 600 μL N-methyl-2-pyrrolidone (NMP) by 30 min sonication to form an ink. Then catalyst ink (100 μL) was loaded on a $10\times 10\text{ mm}^2$ Ni-foam with a catalyst loading of 3.1 mg cm^{-2} . Polarization curves were obtained using linear sweep voltammetry (LSV) with a scan rate of 2 mV s^{-1} . The long-term durability test was performed using chronopotentiometric measurements. Because as-measured reaction currents cannot reflect the intrinsic behaviour of electrocatalysts due to the effect of ohmic resistance, all currents present here are corrected against ohmic potential drop for further analysis.

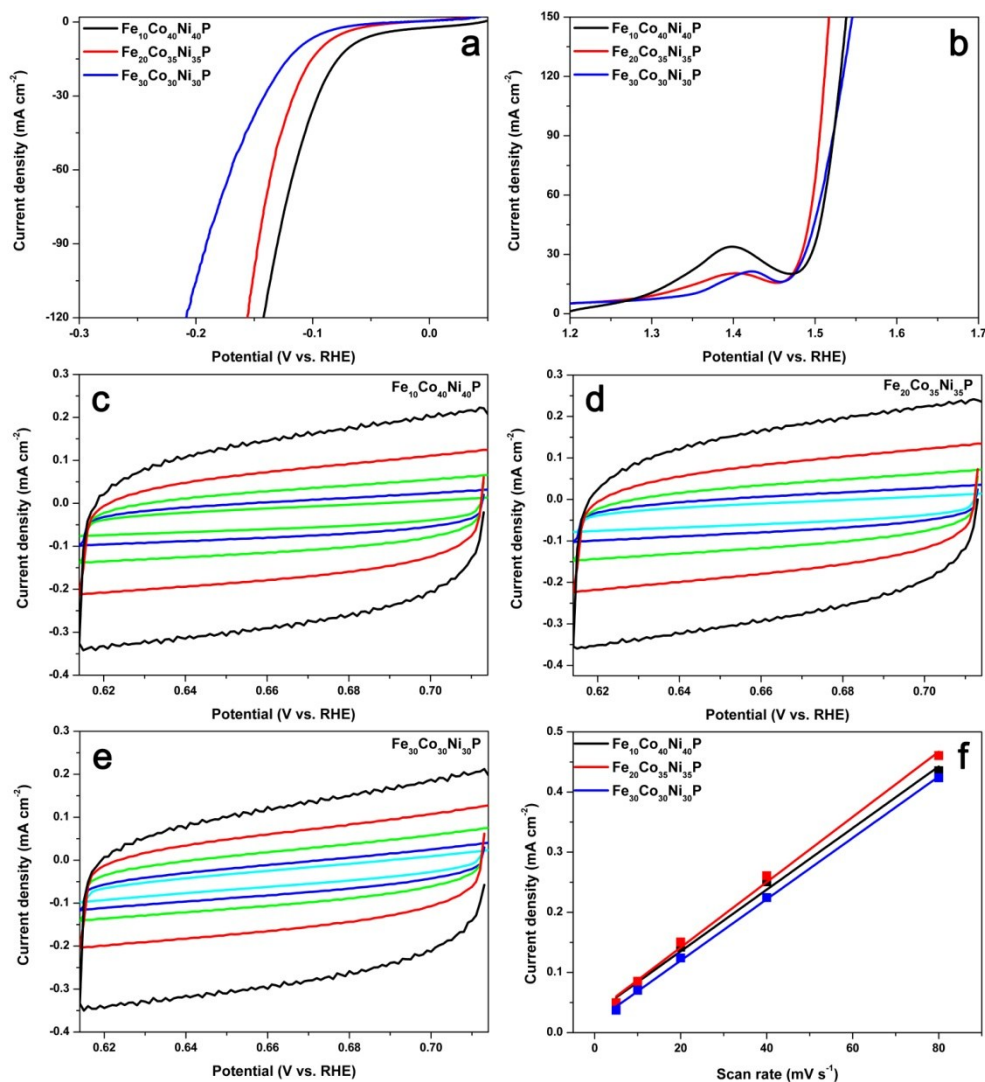


Figure S1. LSV curves for HER (a) and OER (b) of Fe₁₀Co₄₀Ni₄₀P, Fe₂₀Co₃₅Ni₃₅P and Fe₃₀Co₃₀Ni₃₀P with a scan rate of 2 mV s⁻¹ in 1 M KOH. Cyclic voltammograms (c, d, e) at scan rates from 5 to 80 mV s⁻¹. Scan rate dependence of the current densities at 0.66 V vs RHE (f).

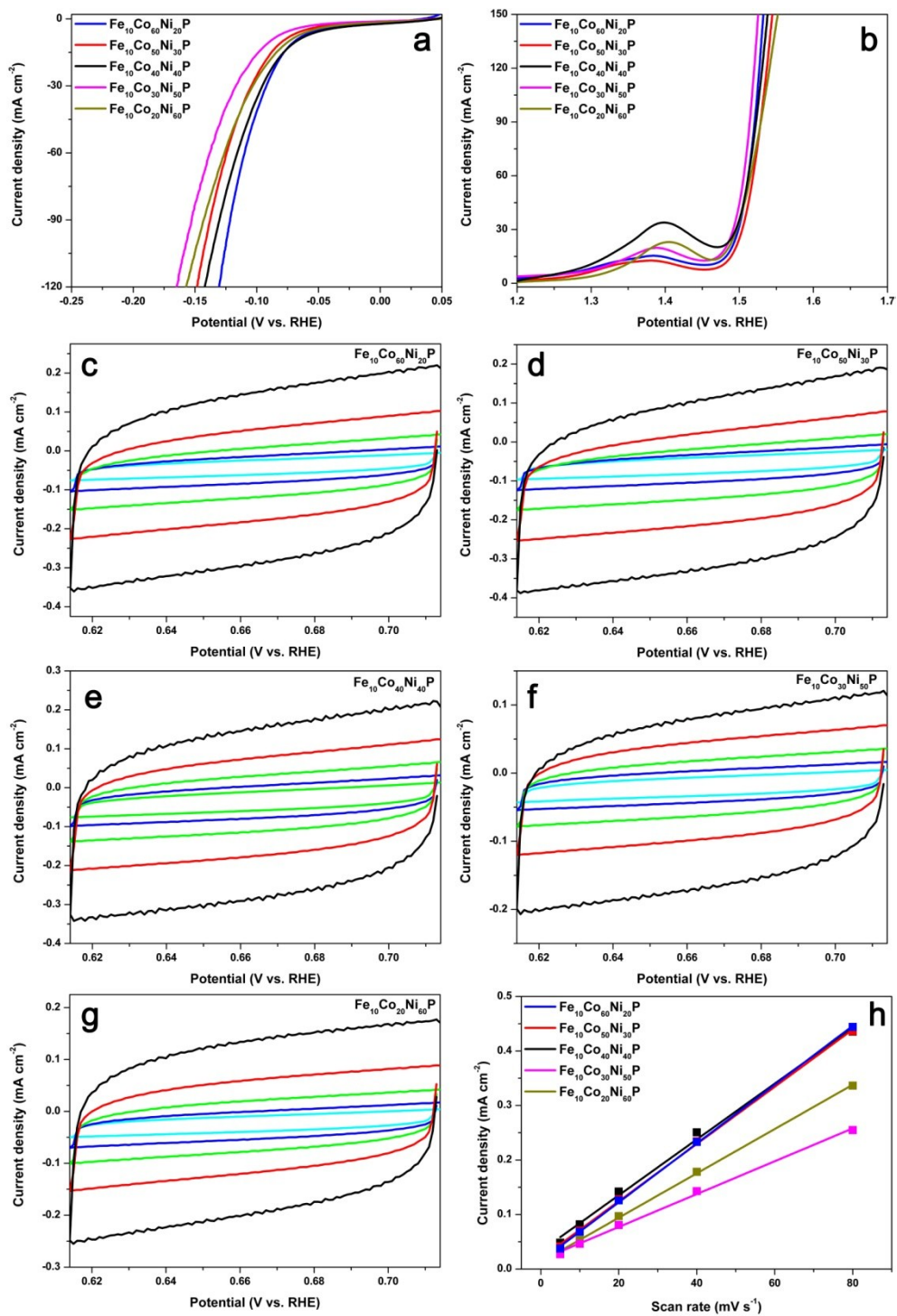


Figure S2. LSV curves for HER (a) and OER (b) of $\text{Fe}_{10}\text{Co}_{60}\text{Ni}_{20}\text{P}$, $\text{Fe}_{10}\text{Co}_{50}\text{Ni}_{30}\text{P}$, $\text{Fe}_{10}\text{Co}_{40}\text{Ni}_{40}\text{P}$, $\text{Fe}_{10}\text{Co}_{30}\text{Ni}_{50}\text{P}$, and $\text{Fe}_{10}\text{Co}_{20}\text{Ni}_{60}\text{P}$ with a scan rate of 2 mV s^{-1} in 1 M KOH. Cyclic voltammograms (c, d, e, f, g) at scan rates from 5 to 80 mV s^{-1} . Scan rate dependence of the current densities at 0.66 V vs RHE (h).

Table S1. ICP-OES data of compositional mole of Fe, Co and Ni in various samples

Catalyst	Fe [mole%]	Co [mole%]	Ni [mole%]
Fe ₃₀ Co ₃₀ Ni ₃₀ P	59	19	13
Fe ₂₀ Co ₃₅ Ni ₃₅ P	35	33	22
Fe ₁₀ Co ₄₀ Ni ₄₀ P	18	47	25
Fe ₁₀ Co ₃₀ Ni ₅₀ P	16	40	34
Fe ₁₀ Co ₂₀ Ni ₆₀ P	14	26	51
Fe ₁₀ Co ₅₀ Ni ₃₀ P	19	55	16
Fe ₁₀ Co ₆₀ Ni ₂₀ P	19	61	10
Fe ₁₈ Co ₇₂ Ni ₀₀ P	26	60	--
Fe ₁₈ Co ₀₀ Ni ₇₂ P	33	--	57
Fe ₀₀ Co ₄₅ Ni ₄₅ P	--	57	33

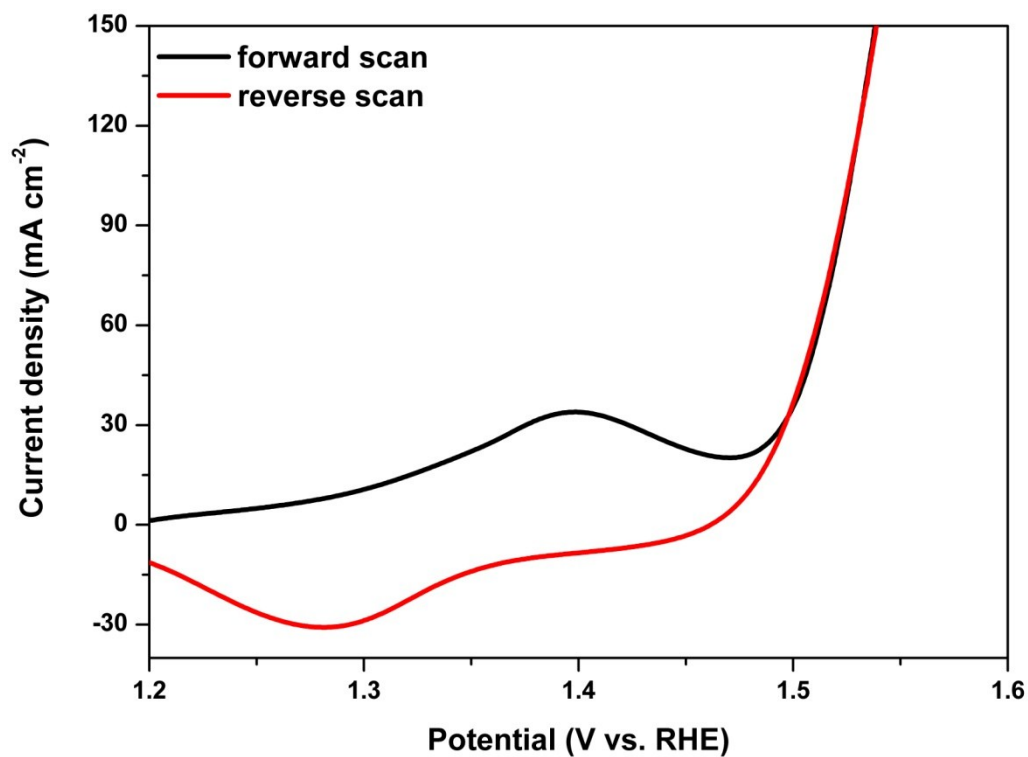


Figure S3. LSV curves of Fe₁₀Co₄₀Ni₄₀P scanning from negative to positive potentials (forward scan) and scanning from positive to negative potentials (reverse scan) in 1 M KOH.

Table S2. Comparison of the electrocatalytic performance of Fe₁₀Co₄₀Ni₄₀P in basic media with other bifunctional full water splitting electrocatalysts.

Catalyst	Water electrolysis test	Current density (10 mA cm ⁻²)	Overpotential (mV)	Reference
Fe ₁₀ Co ₄₀ Ni ₄₀ P	HER	10	68	This work
	OER	10	250	
Ni ₃ S ₂ /NF	HER	10	223	<i>J. Am. Chem. Soc.</i> 2015 , DOI: 10.1021/jacs.5b08186
	OER	10	260	
CoO _x @CN	HER	10	232	<i>J. Am. Chem. Soc.</i> 2015 , 137, 2688-2694
	OER	10	260	
Co-P films	HER	10	94	<i>Angew. Chem. Int.Ed.</i> 2015 , 54, 6251-6254.
	OER	10	345	
Ni ₅ P ₄	HER	10	150	<i>Angew. Chem. Int.Ed.</i> 2015 , 54, 12361-12365.
	OER	10	290	
Co phosphide/ Co phosphate	HER	10	380	<i>Adv. Mater.</i> 2015 , 27, 3175-3180
	OER	10	300	
NiSe Nanowire	HER	10	96	<i>Angew. Chem. Int.Ed.</i> 2015 , DOI: 10.1002/anie.201503407
	OER	20	270	
Ni-NiO/N-rGO	HER	20	160	<i>Adv. Funct. Mater.</i> 2015 , 25, 5799-5808
	OER	10	240	
MnNi _x	HER	10	360	<i>Adv. Funct. Mater.</i> 2015 , 25, 393-399
	OER	10	430	
ultra-small NiFeO _x	HER	10	88	<i>Nat. Commun.</i> 2015 , 6, 7261
	OER	10	250	
NiCo ₂ O ₄ nanowires array	HER	50	263	<i>Nanoscale</i> 2015 , 7, 15122-15126
	OER	20	280	
Ni/N/C	HER	10	190	<i>Adv. Energy Mater.</i> 2015 , DOI: 10.1002/aenm.201401660
	OER	10	390	

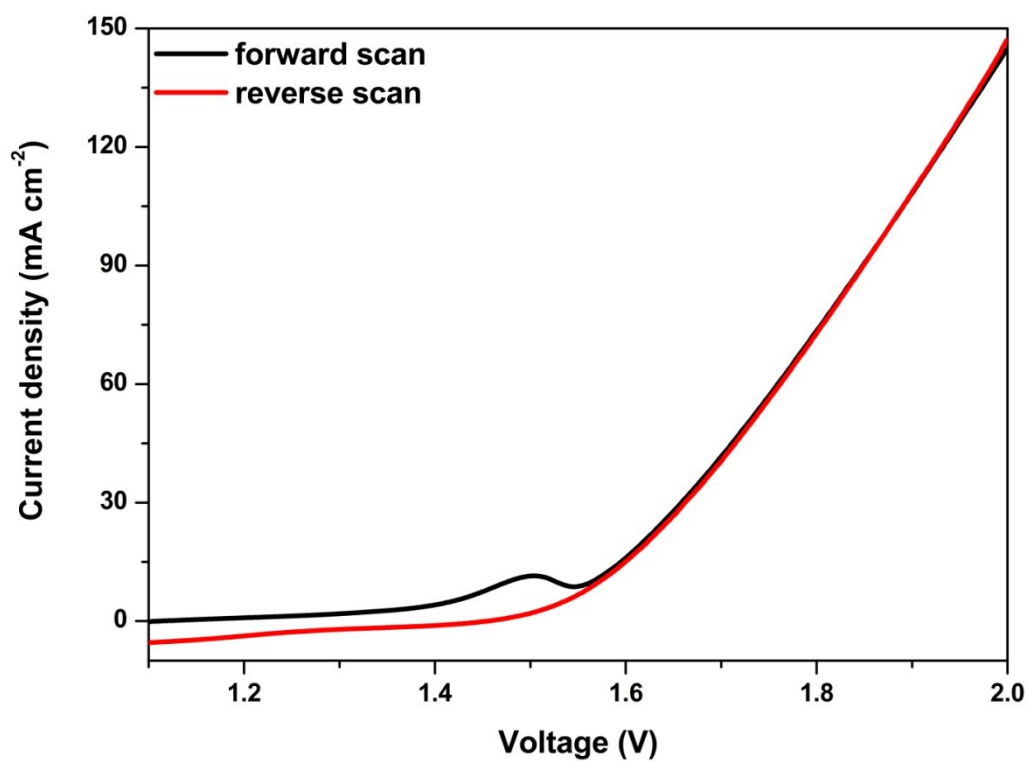


Figure S4. LSV curves of water electrolysis for Fe₁₀Co₄₀Ni₄₀P in a two-electrode configuration scanning from negative to positive potentials (forward scan) and scanning from positive to negative potentials (reverse scan) in 1 M KOH.

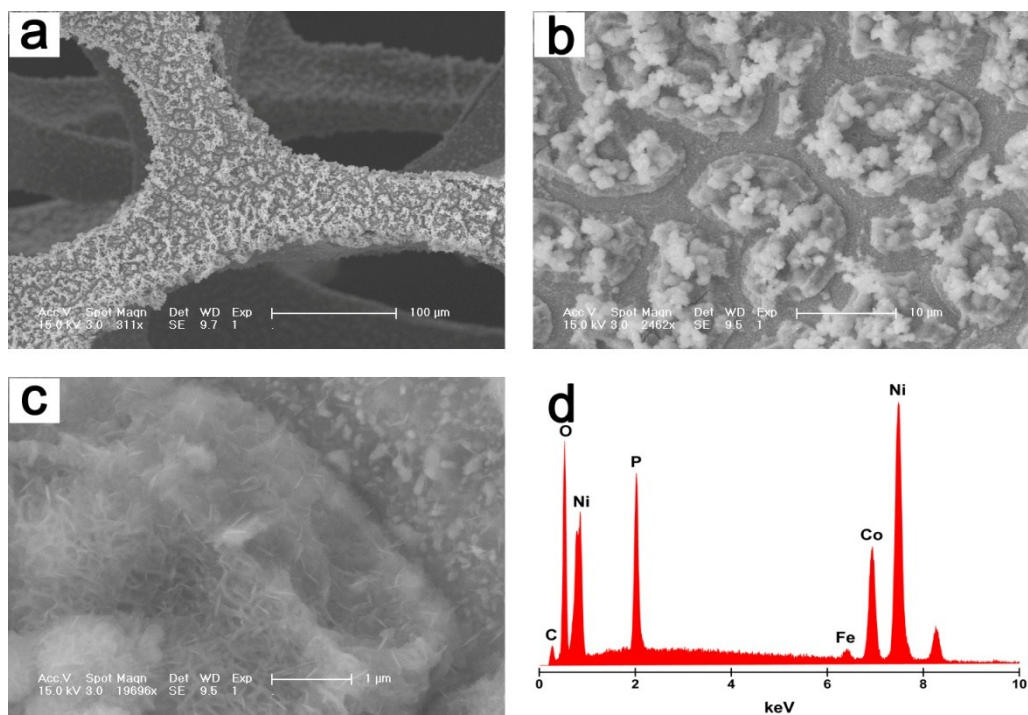


Figure S5. SEM (a-c) images and corresponding EDX (d) spectrum of $\text{Fe}_{10}\text{Co}_{40}\text{Ni}_{40}\text{P}$ after HER test in 1 M KOH.

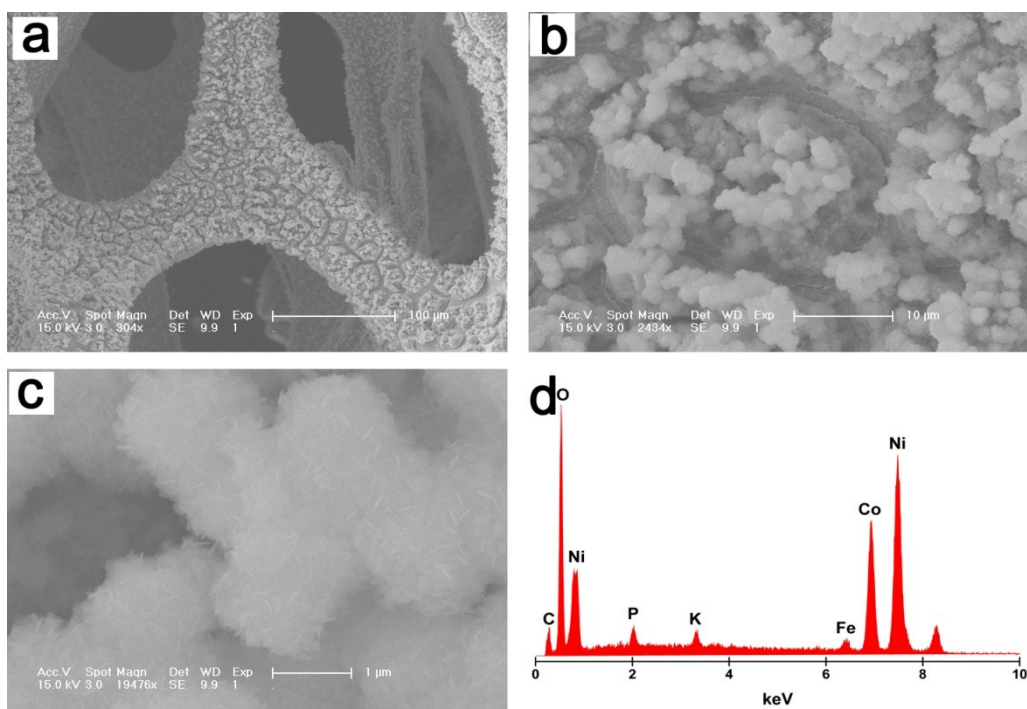


Figure S6. SEM (a-c) images and corresponding EDX (d) spectrum of $\text{Fe}_{10}\text{Co}_{40}\text{Ni}_{40}\text{P}$ after OER test in 1 M KOH.

Table S3. Comparison of the electrocatalytic performance of Fe₁₀Co₄₀Ni₄₀P in neutral media with other electrocatalysts.

Catalyst	Water electrolysis test	Current density (10 mA cm ⁻²)	Overpotential (mV)	Reference
Fe ₁₀ Co ₄₀ Ni ₄₀ P	HER	10	88	This work
	OER	10	466	
H ₂ -NiCat/ O ₂ -NiCat	HER	1.5	452	<i>J. Phy Chem. C</i> , 2014 , 118, 4578-4584
	OER	0.6	618	
Co-NRCNTs	HER	1	330	<i>Angew. Chem. Int.Ed.</i> 2014 , 53, 4372-4376.
CoP/CC	HER	2	65	<i>J. Am. Chem. Soc.</i> 2015 , 137, 7587-7590
Mo ₂ C	HER	1	200	<i>Angew. Chem. Int.Ed.</i> 2012 , 51, 12703-12706.
Co ₃ S ₄ Nanosheets	OER	4	700	<i>Angew. Chem. Int.Ed.</i> 2015 , 54, 12231-12235.
Co ₃ O ₄	OER	0.62	650	<i>Adv. Funct. Mater.</i> 2013 , 23, 227-233
Mn ₃ (PO ₄) ₂ ·3H ₂ O	OER	0.3 _{cat}	260	<i>J. Am. Chem. Soc.</i> 2014 , 136, 7435-7443

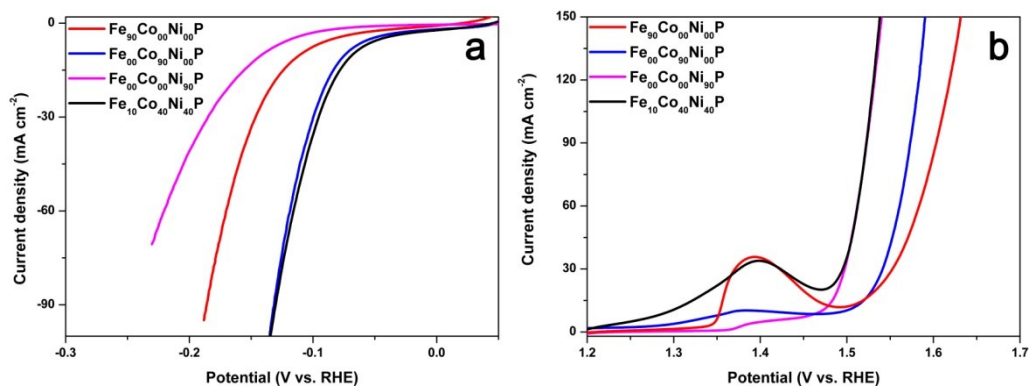


Figure S7. LSV curves for HER (a) and OER (b) of Fe₉₀Co₀Ni₁₀P, Fe₀Co₉₀Ni₁₀P, Fe₀Co₀Ni₉₀P, and Fe₁₀Co₄₀Ni₄₀P with a scan rate of 2 mV s⁻¹ in 1 M KOH.

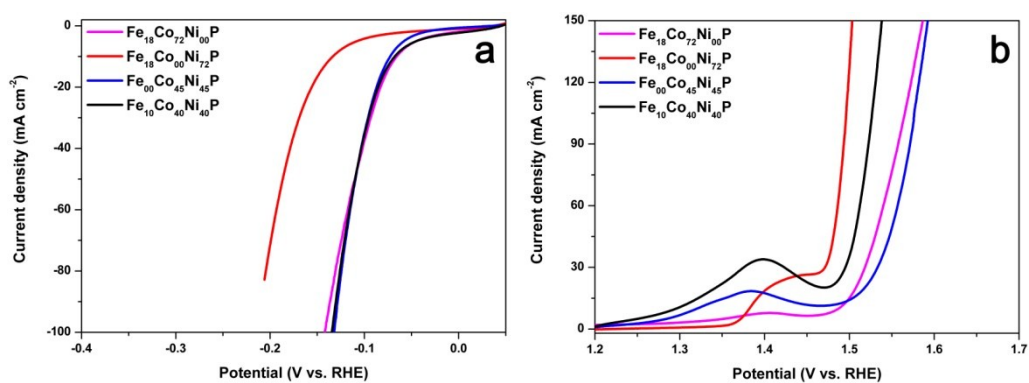


Figure S8. LSV curves for HER (a) and OER (b) of $\text{Fe}_{18}\text{Co}_{72}\text{Ni}_{100}\text{P}$, $\text{Fe}_{18}\text{Co}_{00}\text{Ni}_{72}\text{P}$, $\text{Fe}_{00}\text{Co}_{45}\text{Ni}_{45}\text{P}$, and $\text{Fe}_{10}\text{Co}_{40}\text{Ni}_{40}\text{P}$ with a scan rate of 2 mV s^{-1} in 1 M KOH.

Table S4. Electrocatalytic performance of Fe_xCo_yNi_zP as bifunctional water splitting electrocatalysts.

Catalyst	η_{10} at 10 mA cm ⁻² for HER (mV)	η_{50} at 50 mA cm ⁻² for HER (mV)	η_{10} at 10 mA cm ⁻² for OER (mV)	η_{50} at 50 mA cm ⁻² for OER (mV)
Fe ₃₀ Co ₃₀ Ni ₃₀ P	111	129	230	268
Fe ₂₀ Co ₃₅ Ni ₃₅ P	92	131	234	261
Fe ₁₀ Co ₄₀ Ni ₄₀ P	68	110	250	277
Fe ₁₀ Co ₃₀ Ni ₅₀ P	89	106	242	270
Fe ₁₀ Co ₂₀ Ni ₆₀ P	74	120	245	280
Fe ₁₀ Co ₅₀ Ni ₃₀ P	80	119	252	281
Fe ₁₀ Co ₆₀ Ni ₂₀ P	69	105	250	276
Fe ₁₈ Co ₇₂ Ni ₀₀ P	66	110	257	304
Fe ₁₈ Co ₀₀ Ni ₇₂ P	134	187	230	254
Fe ₀₀ Co ₄₅ Ni ₄₅ P	73	109	279	323
Fe ₉₀ Co ₀₀ Ni ₀₀ P	111	164	292	349
Fe ₀₀ Co ₉₀ Ni ₀₀ P	74	114	268	326
Fe ₀₀ Co ₀₀ Ni ₉₀ P	142	210	241	278